Pharmacogn. Res., 2024; 16(4):757-768.
https://www.phcogres.com

Original Article

Chemical Profiling, Chromatographic Fingerprinting and Anthelmintic Screening of a Rare Species of Holly, *Ilex khasiana* Purkay. from Mizoram, Northeast India

Charles Lalnunfela[1], Pawi Bawitlung Lalthanpuii[2], Hmar Tlawmte Lalremsanga[1], Tochhawng Lalhriatpuii[3], Kholhring Lalchhandama[2,*]

[1]Department of Zoology, Mizoram University, Tanhril, Mizoram, INDIA.
[2]DBT-BUILDER National Laboratory, Department of Life Sciences, Pachhunga University College, Aizawl, Mizoram, INDIA.
[3]Department of Pharmacy, Regional Institute of Paramedical and Nursing Sciences, Zemabawk, Mizoram, INDIA.

ABSTRACT

Background: *I. khasiana* Purkay. is an evergreen tree of the family Aquifoliaceae and is classified critically endangered as only few of them are identified in Northeast India. In Khasi traditional medicine, it is used for the remedy of tuberculosis and viral infections, while it is therapeutically used for all sorts of infections, blood diseases and cancer in the Mizo traditional medicine. As a rare species, there is an overwhelming paucity of knowledge on the chemical and biological properties of this plant. **Objectives:** The study was designed to garner pharmacognostic information on the secondary metabolites in the leaves of *I. khasiana* that are likely the factors behind the medicinal uses and test for an anthelmintic activity using a parasitic helminth model. **Materials and Methods:** *I. khasiana* leaves were collected from Aizawl, Mizoram, India. Five extracts were prepared, namely Petroleum ether (IKP), Chloroform (IKC), Methanol-Hexane (IKM-H) extracts, Methanol-Chloroform (IKM-C) and Methanol-Butanol (IKM-B) extracts. Chemical profiling was done in a single quadrupole Gas Chromatography-Mass Spectrometry (GC-MS). Bioactive compounds were screened using High-Performance Thin-Layer Chromatography (HPTLC) based on nine established bioactive compounds. Anthelmintic assay was performed against a parasitic nematode, *Ascaridia galli*. **Results:** GC-MS data showed that the principal compound was a flavonoid, 7,9-di-tert-butyl-1-oxaspiro[4,5]deca-6,9-diene-2,8-dione from the various extracts. Other major compounds were a terpene lactone, 6-hydroxy-4,4,7a-trimethyl-5,6,7,7a-tetrahydrobenzofuran-2(4H)-one and a phenol, 2,4-di-tert-butylphenol. From HPTLC fingerprinting, two compounds were identified in two extracts, quercetin in IKM-C and β-sitosterol in IKM-H. HPTLC quantification showed that quercetin in IKM-C at an R_f value of 0.49 indicated a total amount of 372.98 ng; while β-sitosterol in IKM-H an R_f value of 0.43 was 257.04 ng. IKM-H with the most diverse compound and containing β-sitosterol, a compound tested for antiparasitic activity, was found to have anthelmintic activity against the helminth model. Scanning electron microscopy revealed anthelmintic effects on the nematode including collapse of the mouth region, contraction throughout the body and localised erosions of the cuticle. **Conclusion:** *I. khasiana* leaf extracts contain important bioactive compounds. The principal flavonoid, lactone and phenol are ostensibly the molecules to be attributed to the medicinal properties. The detections of quercetin and β-sitosterol add to the possible diverse pharmacological properties. The findings directly advocate the necessity for actions into the conservation of this rare and medicinally valuable plant.

Keywords: Anthelmintic activity, Chemical profiling, HPTLC fingerprinting, Nematode, Mizo traditional medicine.

Correspondence:
Prof. Kholhring Lalchhandama
DBT-BUILDER National Laboratory,
Pachhunga University College,
Aizawl-796001, Mizoram, INDIA.
Email: chhandama@pucollege.edu.in

Received: 30-03-2024;
Revised: 20-05-2024;
Accepted: 14-06-2024.

INTRODUCTION

Ilex khasiana Purkay. is an evergreen species of holly belonging to the family Aquifoliaceae and endemic to Northeast India, a region within the Indo-Burma biodiversity hotspot.[1] It was discovered from an isolated specimen in the Khasi Hills of Meghalaya and reported by C. S. Purkayastha, a forest officer under the Government of Assam, in 1938.[2] As only few other specimens could be identified in five localities, the species was declared "rare" in 1983 and then entered in the "Critically Endangered" category of the World Conservation Monitoring Centre in 1998,[3] and subsequently of the IUCN Red List of Threatened Species in 2007.[4] About 3,000 individuals are enumerated surviving in Meghalaya. Although the original specimen was described as a small tree of 4 ft high, many trees of the species can reach up to

DOI: 10.5530/pres.16.4.88

20 m in height.[3] In Khasi ethnomedicine, a concoction of the extracts of the bark and root are acclaimed to be potent curative for tuberculosis and viral infections. In Mizo traditional medicine, the leaves had been known to have healing properties for various pathogenic and helminth infections, blood disorders and cancer. Following remarks from the Mizo traditional healers, a localised distribution was identified from Mizoram and reported in 2019.[5] Pharmacological screening indicated that the leaf extract indeed exhibits antiparasitic activity against intestinal tapeworms,[6] as well as anti-inflammatory and analgesic activities in rodent models.[7]

The genus *Ilex* is itself a fascinating group as it represents the sole extant members of the family Aquifoliaceae. There are 669 species documented mostly from Asia and South America, many of them widely used in traditional medicines with at least 38 of them in cancer therapy.[8] In different parts of South America, species such as *I. paraguariensis, I. argentina, I. brasiliensis, I. brevicuspis, I. dumosa, I. integerrima, I. microdonta, I. pseudobuxus, I. taubertiana* and *I. theezans* are popularly used as health drinks and alternatives to tea. The health benefits are believed to be related to prevention of cancer development.[9] *I. paraguariensis* is the most popular herbal tea, known as yerba mate, cherished for its rich caffeine and is the most pharmacologically investigated.[10] It is determined to be a rich source of bioactive phytocompounds including caffeoyl derivatives (caffeic acid, chlorogenic acid, 3,4-dicaffeoylquinic acid, 3,5-dicaffeoylquinic acid and 4,5-dicaffeoylquinic acid) and flavonoids (quercetin, kaempferol and rutin).[11] These are secondary metabolites which are already documented for their antioxidant, hence, cancer preventive and direct cytotoxic activity against different cancer cell lines.[12] The crude extract of *I. paraguariensis* has been demonstrated for anticancer activity against adenocarcinomic human alveolar basal epithelial (A549 cells), Caucasian Oesophageal carcinoma (OE-33 cells),[13] Human Colon adenocarcinoma (HT-29 and CaCo-2 cells) and urinary bladder carcinoma cells (T24).[14]

In traditional Chinese medicine, 20 species of *Ilex* are used for different diseases.[9] *I. kudingcha* and *I. latifolia* are used as a popular herbal tea, called *kudingcha* and are known to be a remedy for arteriosclerosis, common cold, eye infections, cancer, cardiovascular disorders, cerebrovascular diseases, diabetes, diarrhoea, dysentery, hypertension, pharyngitis and rhinitis.[15,16] *I. pubescens* is used in the treatment of bronchial asthma, coronary artery disease, hepatitis, high cholesterol and hypertension. Its bioactive metabolites have been shown to have anticancer, analgesic, anti-inflammatory, anticlotting and neuro-protective activities.[17] *I. cornuta* is used for the treatment of headache, toothache, bloodshot eyes and tinnitus. It contains many glycosides, flavonoids, phenols, saponins and triterpenes, some of which are novel compounds that are experimentally tested for anticancer,[18,19] antimicrobial, anti-inflammatory, antidiabetic, antiulcer and hypolipidemic activities.[20,21] In the light of these information, the poor understanding of its medicinal values and its endangered nature, it is of prime importance to conduct systematic chemical and pharmacological analyses of *I. khasiana* to appreciate the true pharmacological potentials.

MATERIALS AND METHODS

Chemicals

All chemicals were standard analytical grades procured from HiMedia Laboratories Private Limited, Mumbai, India; except acetonitrile, silica gel, methanol and absolute alcohol that were obtained from Sigma-Aldrich Chemicals Pvt., Ltd, Bangalore, India. Albendazole (Zenlee) was a product of UNI-PEX Pharmaceutical Private Limited, New Delhi, India.

Plant identification and extraction

I. khasiana was collected from Luangmual, a locality within Aizawl, Mizoram, India, located at 23°44.556'N and 92°41.956'E (Figure 1). A herbarium specimen was identified at the Botanical Survey of India, Eastern Regional Office, Shillong, Meghalaya and is maintained at the Department of Pharmacy, Regional Institute of Paramedical and Nursing Sciences, Zemabawk, Mizoram, India, with catalogue number BSI/EC/Tech./2008/577. Additional authentication was done from the Royal Botanic Gardens, Kew (taxon code 83411-1 on https://powo.science.kew.org) and The Plant List (taxon code 2860918 on http://www.theplantlist.org). The leaves were washed in distilled water and dried in shade at a room temperature (24±1°C). The dried samples were loaded to a 5 L Soxhlet apparatus for extraction using three solvents of varying polarities, namely petroleum ether (polarity index 0.1), chloroform (polarity index 0.26) and methanol (polarity index 0.76). Extraction was run for 72 hr in each solvent. The extracts were concentrated by evaporating and recovering the solvent in a rotary vacuum evaporator (Buchi Rotavapor® R-215, Flawil, Switzerland).

The crude extract from the most polar solvent, methanol, contained numerous compounds and was fractionated into three extracts to yield better compound separation using butanol (polarity index 0.586), chloroform (polarity index 0.259) and hexane (polarity index 0.009). In brief, equal volumes of the crude extract and the fractionating solvents were mixed in a separating funnel. After continuous reflux for 4 hr, the solutions formed a clear partition in between so that the bottom and upper solutions were collected separately. The fractions were concentrated in rotary vacuum evaporator. After complete fractionation, five extracts were obtained, namely the Petroleum ether (hereafter denoted as IKP), Chloroform (IKC), Methanol-Hexane (IKM-H), Methanol-Chloroform (IKM-C) and Methanol-Butanol (IKM-B) extracts.

GC-MS profiling

Chemical compounds were analysed in a single quadrupole gas chromatography-mass spectrometry using Thermo Scientific TRACE™ 1300 ISQ™ LT (Waltham, USA). Methanol was used to dissolve the extracts and obtain 50 mg/mL of a working concentration for each extract. Each sample was loaded with five plunger strokes to obtain 1 µL of the targeted sample. The stationary phase consisted of non-polar column TR-5MS having a dimension of 30 m length×0.25 mm width×0.25 µm film thicknesses. The carrier gas, helium was injected at 1 mL/min in a splitting ratio of 1:50. The oven temperature was set at 70°C and an incrementally increased at 10°C for 10 min each step up to 250°C. Ion source and transfer line temperature were set at 220°C. The mass spectrometer was run for 32 min covering the range of 10 to 1,100 amu. Chemical data was generated from Thermo Scientific™ Xcalibur™ software. Compounds were identified based on their chemical formulae, retention times and molecular masses from the chemical libraries of Wiley Registry™ and National Institute of Standards and Technology.

High-Performance Thin-Layer Chromatography

Chemical fingerprinting and quantification were done using HPTLC.[22] Standard natural metabolites including asiatic acid (triterpene), boswellic acid (triterpene), chebulagic acid (tannin), chlorogenic acid (caffeic acid ester), ellagic acid (phenol), ferulic acid (phenol), gallic acid (phenol), quercetin (flavonoid) and β-sitosterol (steroid) were used for reference. 1 mg of each compound was dissolved in 1000 µL of methanol to get a stock solution for each reference. Each stock solution was diluted with methanol to obtain a working concentration of 50 µg/mL for each compound.

For chromatographic separation, pre-coated Thin-Layer Chromatography (TLC) plates on a support aluminium sheet with silica gel 60 coupled with fluorescence indicator F_{254} (Merck KGaA, Darmstadt, Germany), having layer thickness of 250 µm and size 20×10 cm were used as the stationary phase. 5 µL of the five *I. khasiana* extracts were spotted in 10 mm bands on individual TLC plates using Linomat 5 applicator attached to CAMAG® HPTLC system (Muttenz, Switzerland). The plates were developed in CAMAG® twin-trough chamber using the appropriate mobile phases as shown in Table 1. The plates were removed and allowed to air-dry when the solvent front reached 7 cm. Compounds were scanned in CAMAG® TLC Scanner 4 at the appropriate wavelength using winCATS software (Cordial Versicherungs-Dienstleistungen GmbH, Hannover, Germany) to obtain the extract fingerprints in the form of chromatograms.

Calibration and quantification of quercetin

The working solutions of standard compounds were applied on TLC plates at 2, 4, 6, 8, 10, 12 and 14 µL to obtain seven-point linear calibration curves. Application was done at the speed of 150 nL/sec. 4 µL of *I. khasiana* extract (prepared at 50 mg/mL) was similarly applied on a TLC plate. The twin-trough developing chamber was pre-saturated with 20 mL of toluene:ethyl acetate:formic acid (5:4:0.2 v/v/v) as a mobile phase for 15 min and the TLC plates were developed up to a height of 7 cm. The plates were visualised under ultraviolet chamber using CAMAG® Smart DIGI. Quantitative evaluation of the plate was performed in the TLC scanner with the conditions: 254 nm wavelength; slit width 5×0.45 mm, scanning speed 40 mm/sec and data resolution 50 µm/step using deuterium lamp.

Calibration and quantification of β-sitosterol

A winCATS planar chromatography manager software (version 1.4.5) was used to apply 10 standard levels containing 100 to 550 ng of β-sitosterol. Plant extracts (50 mg/mL) were applied on TLC plates at 150 nL/sec using nitrogen as the spray gas. The developing chamber was saturated with toluene:methanol (16:2 v/v). The plates were removed after the solvent front reached 7 cm. The plate derivatization was performed by spraying the TLC plate with anisaldehyde sulphuric acid and placed in an oven at 100°C until prominent bands appeared. The plates were then scanned using the conditions: 366 nm wavelength; slit dimension 5×0.45 mm, scanning speed 40 mm/sec and data resolution 100 µm/step.

Validation of HPTLC method

The methods that were used for validation were performed following the International Conference on Harmonization guidelines.[23]

Linearity

14 different concentrations of the standard compounds were prepared for linearity studies (n=14). Peak area was measured and taken as a response. The plate was then developed by using mobile phase. The peak area was plotted against concentrations for the calibration curve.

Limit of Detection and Limit of Quantification

For the evaluation Limit of Detection (LOD) and Limit of Quantification (LOQ) different concentrations of the standard stock solutions were applied to determine the following equation.

$$\text{LOD} = \frac{3.3 \times \text{Standard deviation of the y intercept}}{\text{Slope of the calibration curve}}$$

$$\text{LOQ} = \frac{10 \times \text{Standard deviation of the y intercept}}{\text{Slope of the calibration curve}}$$

Recovery

For percent recovery, known concentrations of standards were added to a pre-analysed sample. The spiked samples were then analysed by the prescribed HPTLC method.[22]

Anthelmintic susceptibility assay

Anthelmintic activity was evaluated on a nematode, *Ascaridia galli* Schrank, 1788, an intestinal helminth of fowl, *Gallus gallus* Linnaeus, 1758, based on helminth survival assay.[24] A reference anthelmintic drug, albendazole (at manufactured dosage 20 mg/mL) was used to compare the anthelmintic efficacy of *I. khasiana* extract at the same concentration. The nematodes were maintained in a culture medium (composed of 0.9% neutral phosphate-buffered saline supplemented with 1% dimethyl sulfoxide) at 37±1°C in a microbiological incubator. Negative control was maintained in a culture medium only. Anthelmintic efficacy was determined by Student's *t*-test against the negative control with the level of significance taken at $p<0.05$. The nematodes were processed for scanning electron microscopy following the standardised method for helminths.[25] The cestodes were first fixed in 10% neutral-buffered formaldehyde, post-fixed in osmium tetroxide, dehydrated in acetone, stabilised in tetramethylsilane, coated with gold in JFC-1100 ion sputter and finally observed under a JSM-6360 scanning electron microscope (JEOL Ltd., Tokyo, Japan).

RESULTS

Chemical profiling

Chemical compounds identified in the leaf extracts of *I. khasiana* from the most non-polar solvent, i.e., IKP, are given in Table 1, based on the gas chromatogram and mass spectra (Supplementary Figure 1). 13 different compounds were identified. The most abundant compound was 7,9-di-tert-butyl-1-oxaspiro[4,5]deca-6,9-diene-2,8-dione (at relative abundance of 92.56%). At above the threshold of high occurrence, the second-most abundant was 6-hydroxy-4,4,7a-trimethyl-5,6,7,7a-tetrahydrobenzofuran-2(4H)-one (83.83%), followed by 2,4-di-tert-butylphenol (69.77%) and n-hexadecanoic acid (63.19%). In the extract from the medium polarity, i.e., IKC, 11 different compounds were confirmed (Supplementary Figure 2). 7,9-di-tert-butyl-1-oxaspiro (4,5)deca-6,9-diene-2,8-dione (86.41%) dominated the total compounds, followed by 2,4-di-tert-butylphenol (73.26%) (Table 2). IKM, extracted with the most polar solvent, showed a long list of compounds and was separated into fractions for a coherent identification of the compound. There were 18 distinct compounds in IKM-H (Table 3, Supplementary Figure 3), 8 in IKM-C (Table 4, Supplementary Figure 4) and 11 in IKM-B (Table 5, Supplementary Figure 5). 2,4-Di-tert-butylphenol was the only common major compounds in all the three fractions, with 72.45% relative abundance in IKM-H, 36.23% in IKM-C and 70.74% in IKM-B. However, 7,9-di-tert-butyl-1-oxaspiro(4,5)deca-6,9-diene-2,8-dione was the principal compound in IKM-C (85.38%) and IKM-B (81.27%), but absent in IKM-H. n-Hexadecanoic acid was in high amount in IKM-H (63.95%) and IKM-B (64.02%), but not detect in IKM-C.

HPTLC fingerprinting

HPTLC fingerprinting of *I. khasiana* extracts performed with reference to nine bioactive compounds is shown in Table 6. Asiatic acid, boswellic acid, chebulagic acid, chlorogenic acid, ellagic acid, ferulic acid and gallic acid were not detected in any

Table 1: Compounds identified in *I. khasiana* Petroleum ether extract (IKP) from GC-MS.

Sl. No.	Retention time (min)	Relative abundance (%)	Compound	Formula	Molecular mass
1	17.65	20.59	2-Buten-1-one, 1-(2,6,6-trimethyl-1-cyclohexen-1-yl).	$C_{13}H_{20}O$	192
2	17.88	69.77	2,4-Di-tert-butylphenol	$C_{14}H_{22}O$	206
3	18.31	38.32	2(4H)-Benzofuranone, 5,6,7,7a-tetrahydro-4,4,7a-trimethyl.	$C_{11}H_{16}O_2$	180
4	20.99	83.83	6-Hydroxy-4,4,7a-trimethyl-5,6,7,7a-tetrahydrobenzofuran-2(4H)-one.	$C_{11}H_{16}O_3$	196
5	21.18	41.25	5,5,8a-Trimethyl-3,5,6,7,8,8a-hexahydro-2H-chromene.	$C_{12}H_{20}O$	180
6	22.49	92.56	7,9-Di-tert-butyl-1-oxaspiro (4,5) deca-6,9-diene-2,8-dione.	$C_{17}H_{24}O_3$	276
7	22.82	63.19	n-Hexadecanoic acid.	$C_{16}H_{32}O_2$	256
8	23.09	44.87	Hexadecanoic acid, ethyl ester.	$C_{16}H_{36}O_2$	284
9	24.25	38.34	3,7,11,15-Tetramethyl-2-hexadecen-1-ol.	$C_{16}H_{40}O$	296
10	24.51	40.68	9,12,15-Octadecatrienoic acid.	$C_{18}H_{30}O_2$	278
11	24.66	47.39	Octadecanoic acid.	$C_{18}H_{36}O_2$	284
12	25.18	23.99	3,7,11,15-Tetramethyl-2-hexadecen-1-ol.	$C_{20}H_{40}O$	296
13	31.37	42.38	Squalene.	$C_{30}H_{50}$	410

of the five extracts. Quercetin and β-sitosterol were detected in the methanol fractions at the wavelengths of 254 and 366 nm respectively. However, quercetin was detected only in IKM-C, while β-sitosterol was detected in IKM-H.

Quantification of quercetin

IKM-C, the only extract that showed the presence of quercetin from HPTLC fingerprinting, was analysed for quantification. Comparison of the plant extract and standard compound was done using toluene:ethyl acetate:formic acid (5:4:0.2 v/v/v) as a mobile phase (Table 6). The chromatogram (Figure 2A) showed the precision of the mobile phase used and the sensitivity of methods employed as shown in Table 7. A steady seven-point linear calibration curve was obtained against 2, 4, 6, 8, 10, 12 and 14 µL of quercetin at 100-500 ng/band for which the correlation coefficient was determined at 0.97 between the standard compound and IKM-C. The reliability of the chromatography was additionally attested by high recovery value, with IKM-C showing >97.5% mean recovery (Table 8). The lowest amount at which the compound can be detected, the Limit of Detection (LOD) was calculated as 68.01 ng/band, while the lowest quantifiable amount, the Limit of Quantification (LOQ) was as low as 206.07 ng/band. Quercetin in IKM-C showed an R_f value of 0.49, corresponding to that of the standard compound (Supplementary Figures 6 and 7) and the total amount of quercetin quantified in the extract was 372.98 ng (Table 9).

Quantification of β-sitosterol

As HPTLC fingerprinting showed that β-sitosterol was detectable on in IKM-H, which was then processed for quantification. Chromatographic migration was done in toluene: methanol (16:2 v/v) as the mobile phase (Table 6). The calibration curve was linear at 100-550 ng/band for ten-level calibration curve (Figure 2B) with a correlation coefficient of 0.99 (Table 7). The mean recovery percentages were all higher than 97 for all the test samples (Table 8). The quantifiable limits were 42.99 ng/band for LOD and 143.28 ng/band for LOQ. β-sitosterol was determined at an R_f value 0.43 in IKM-H as that of the standard compound (Supplementary Figures 8 and 9) and the total amount present in IKM-H was 257.04 ng (Table 9).

Anthelmintic activity

Comparison of the survival of *A. galli* in control media and treatment with IKM-H is shown in Table 10. The plant extract and albendazole at 20 mg/mL each indicated significant anthelmintic activity. Survival time was normalised against that of the nematodes maintained in the negative control. Survival time indicated 4.48±0.98 hr (mean±standard deviation) in albendazole and 22.21±2.85 hr in IKM-H treatments. From scanning electron micrographs, the nematode on its anterior region showed three radiating lips from the central mouth region (Figure 3A). The surrounding neck region is highly convoluted and deflated that indicates breakdown of the cuticular layer. A single lip revealed complete disintegration of the denticles into spongy mass of tissues (Figure 3B). The mouth tissue also tattered forming lumps of debris (Figure 3C). The general body indicated extensive shrinkage of the cuticle (Figure 4A), with patches of erosion and scarring (Figure 4B). The cuticular collapse extended to the extreme posterior end with the tail piece crooked (Figure 4C).

Table 2: Compounds identified in *I. khasiana* Chloroform extract (IKC) from GC-MS.

Sl. No.	Retention time (min)	Relative abundance (%)	Compound	Formula	Molecular mass
1	13.10	18.19	Docosahexaenoic acid, 1,2,3-propanetriyl ester	$C_{69}H_{98}O_6$	1022
2	14.75	15.49	Benzoxazol, 2,3-dihydro-2-thioxo-3-diallylaminomethyl.	$C_{14}H_{16}N_{2O}S$	260
3	17.14	13.20	Morphinan-4,5-epoxy-3,6-di-ol, 6-[7-nitrobenzofurazan-4-yl]amino.	$C_{26}H_{27}N_5O_6$	505
4	17.88	73.26	2,4-Di-tert-butylphenol.	$C_{14}H_{22}O$	206
5	21.18	19.35	-4-Hydroxy-3,5,5-trimethyl-4-(3-oxobut-1-en-1-yl) cyclohex-2-enone.	$C_{13}H_{18}O_3$	222
6	22.42	16.28	Oxiraneundecanoic acid.	$C_{19}H_{36}O_3$	312
7	22.49	86.41	7,9-Di-tert-butyl-1-oxaspiro(4,5) deca-6,9-diene-2,8-dione.	$C_{17}H_{24}O_3$	276
8	24.74	15.65	Octadecane, 3-ethyl-5-(2-ethylbutyl).	$C_{26}H_{54}$	366
9	26.45	11.25	9-Octadecenoic acid, (2-phenyl-1,3-dioxolan-4-yl) methyl ester.	$C_{28}H_{44}O_4$	444
10	29.55	11.76	Arsenous acid, tris(trimethylsilyl) ester.	$C_9H_{27}AsO_3Si_3$	342
11	30.72	12.35	Tris(tert-butyldimethylsilyloxy)arsane.	$C_{18}H_{45}AsO_3Si_3$	468

Table 3: Compounds identified in *I. khasiana* Methanol-Hexane extract (IKM-H) from GC-MS.

Sl. No.	Retention time (min)	Relative abundance (%)	Compound	Formula	Molecular mass
1	16.40	11.42	2-Myristynoyl pantetheine	$C_{25}H_{44}N_2O_5S$	484
2	17.15	13.46	1,4-Diaminonaphthalene	$C_{10}H_{10}N_2$	158
3	17.88	72.45	2,4-Di-tert-butylphenol	$C_{14}H_{22}O$	206
4	18.55	64.05	Benzene, (1-ethyloctyl)	$C_{16}H_{26}$	218
5	18.98	52.66	Benzene, (1-methylnonyl)	$C_{16}H_{26}$	218
6	20.15	42.42	Benzene, (1-methyldecyl)	$C_{17}H_{28}$	232
7	20.47	59.80	Benzene, (1-butyloctyl)	$C_{18}H_{30}$	246
8	21.27	43.58	Benzene, (1-methylundecyl)	$C_{18}H_{30}$	246
9	22.23	30.36	Benzene, (1-methyldodecyl)	$C_{19}H_{32}$	260
10	22.42	41.92	Hexadecanoic acid, methyl ester	$C_{17}H_{34}O_2$	270
11	22.76	63.95	n-Hexadecanoic acid	$C_{16}H_{32}O_2$	256
12	24.14	14.75	9,12,15-Octadecatrienoic acid, methyl ester	$C_{19}H_{32}O_2$	292
13	24.48	16.84	Cyclopropaneoctanoic acid, 2-[[2-[(2-ethylcyclopropyl) methyl]cyclopropyl]methyl]	$C_{22}H_{38}O_2$	334
14	25.34	23.20	2,3-Dimethyl-1,4,4a,9a-tetrahydroanthracene-9,10-dione	$C_{16}H_{16}O_2$	240
15	26.87	20.55	Ethyl iso-allocholate	$C_{26}H_{44}O_5$	436
16	27.67	18.76	9-Octadecenoic acid, (2-phenyl-1,3-dioxolan-4-yl) methyl ester	$C_{28}H_{44}O_4$	444
17	28.45	16.32	1,25-Dihydroxyvitamin D_3	$C_{30}H_{52}O_3Si$	488
18	28.70	15.69	Androstane-11,17-dione, 3-[(trimethylsilyl)oxy]-, 17-[O-(phenylmethyl)oxime]	$C_{29}H_{43}NO_3Si$	481

Table 4: Compounds identified in *I. khasiana* Methanol-Chloroform extract (IKM-C) from GC-MS.

Sl. No.	Retention time (min)	Relative abundance (%)	Compound	Formula	Molecular mass
1	17.71	36.23	2,4-Di-tert-butylphenol.	$C_{14}H_{22}O$	206
2	20.88	17.42	Fumaric acid, 2-(2-methoxyethyl)hexyl 2,3-dichlorophenyl ester.	$C_{19}H_{24}Cl_2O_5$	402
3	21.18	41.88	5,5,8a-Trimethyl-3,5,6,7,8,8a-hexahydro-2H-chromene.	$C_{12}H_{20}O$	180
4	22.49	85.38	7,9-Di-tert-butyl-1-oxaspiro(4,5) deca-6,9-diene-2,8-dione.	$C_{17}H_{24}O_3$	276
5	24.66	23.06	2-Bromotetradecanoic acid.	$C_{14}H_{27}BrO_2$	306
6	28.39	16.43	Lupeol	$C_{30}H_{50}O$	426
7	30.44	16.59	1-Heptatriacotanol	$C_{37}H_{76}O$	536
8	30.66	12.46	Androstane-11,17-dione, 3-[(trimethylsilyl)oxy]-, 17-[O-(phenylmethyl)oxime].	$C_{29}H_{43}NO_3Si$	481

DISCUSSION

The identifications of 7,9-di-tert-butyl-1-oxaspiro [4,5]deca-6, 9-diene-2, 8-dione, 6-hydroxy-4,4, 7a-trimethyl- 5,6,7,7a-tetrahydrobenzofuran-2 (4H)-one, 2,4-di-tert-butylphenol and hexadecanoic acid in *I. khasiana* are fascinating as they can be attributed the claimed traditional uses of the plant. 7,9-Di-tert-butyl-1-oxaspiro (4,5)deca-6,9-diene-2,8-dione is a flavonoid commonly found in the essential oils of several plants. It is a major component of *Ficus benghalensis* which reportedly is an anti-platelet, anti-thrombotic and thrombolytic source.[26] It apparently contributes to the high antioxidant and anti-inflammatory activities of *Nitzschia palea*[27] and *Tamarindus indica*.[28] 6-Hydroxy-4,4,7a-trimethyl-5,6,7,7a-tetrahydrobenzofuran-2(4H)-one is a terpene lactone which is attributed to the anticancer and antimicrobial activities of *Glycosmic cyanocarpa*.[29] Isolated from *Sargassum horneri*, the compound downregulates inflammatory mediators such as inducible nitric oxide synthase and cyclooxygenase-2 and pro-inflammatory cytokine like prostaglandin E_2.[30] *Octoblepharum albidum*'s antidiabetic property was demonstrated to be due to the terpene lactone as the isolated compound was shown to inhibit α-glucosidase and α-amylase.[31] 2,4-Di-tert-butylphenol is cytotoxic phenol produced by a wide range of organisms from bacteria, protists, fungi, plants to animals and is established to have antibacterial, antifungal, anticancer, anthelmintic and antiviral activities.[32] However, it is an unstable chemical for pharmaceutical formulation. Instead, its potent bioactivity is exploited in the syntheses of several anticancer compounds using it as a functional moiety.[33,34] Hexadecanoic acid is shown to have anti-inflammatory,[35] anticancer[36] and antibacterial activities.[37]

(A)

(B)

Figure 1: *Ilex khasiana* naturally growing at Luangmual, Aizawl, Mizoram. The tree (left) near a construction site from which its leaves (right) were collected and used for the study (Photo: Lalnunfela).

(A)

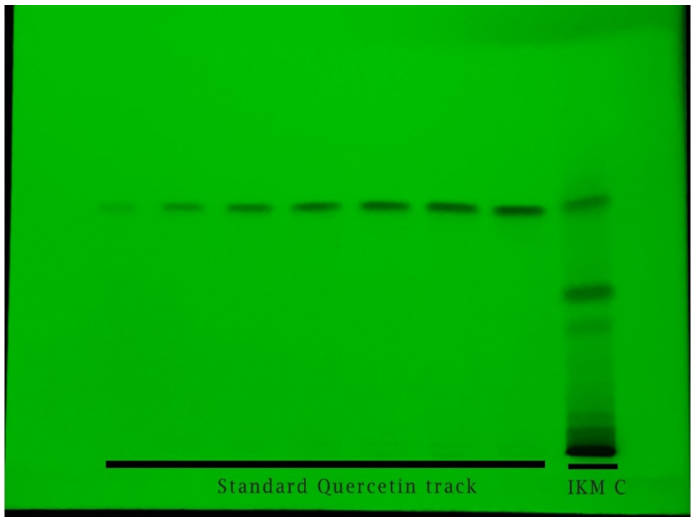

(B)

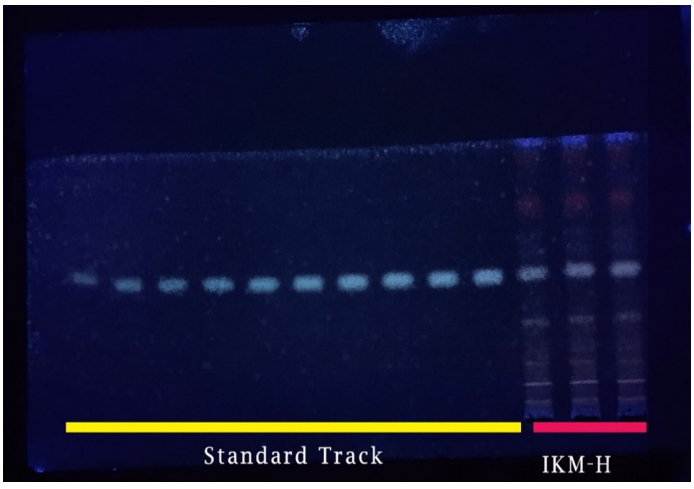

Figure 2: CAMAG® TLC Scanner 4 image of TLC plate showing the separation of *I. khasiana* extracts. (A) Methanol-chloroform extract (IKM-C) with seven-level concentration of quercetin. (B) Methanol-hexane extract (IKM-H) with ten-level concentrations of β-sitosterol.

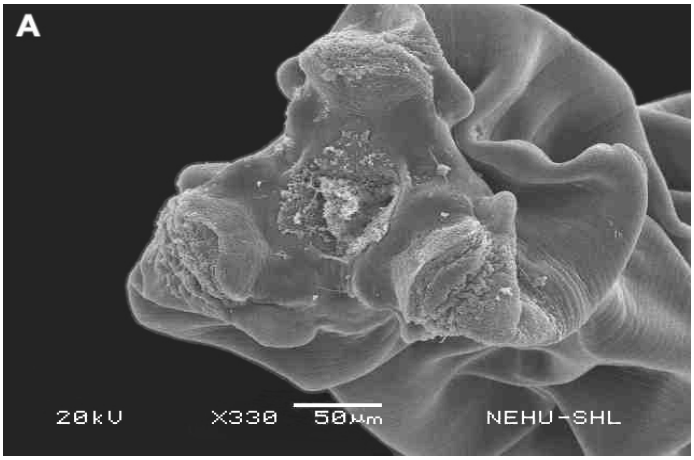

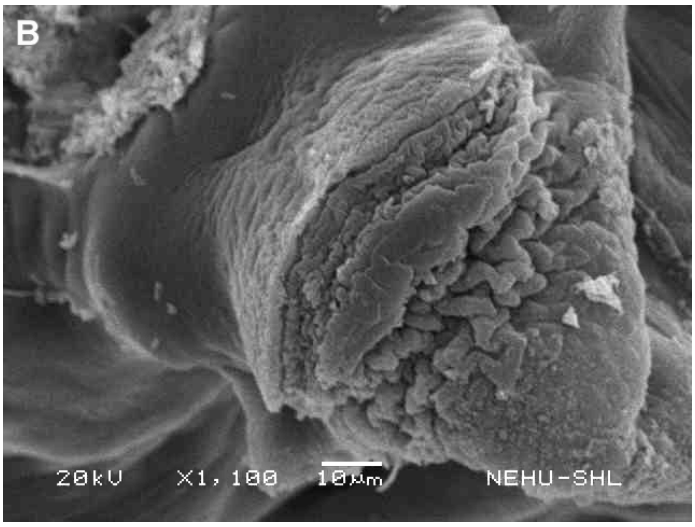

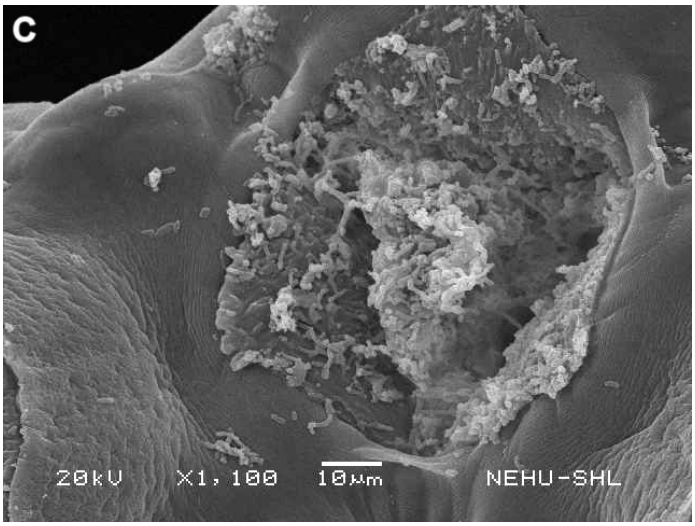

Figure 3: Scanning electron micrograph of *A. galli* treated with 20 mg/mL of *I. khasiana* methanol-hexane extract (IKM-H). (A) Anterior region of the body showing three lips and a central mouth. (B) A single lip showing loss of denticles and formation of tissue lumps. (C) Magnification of the mouth indicated tissue damages.

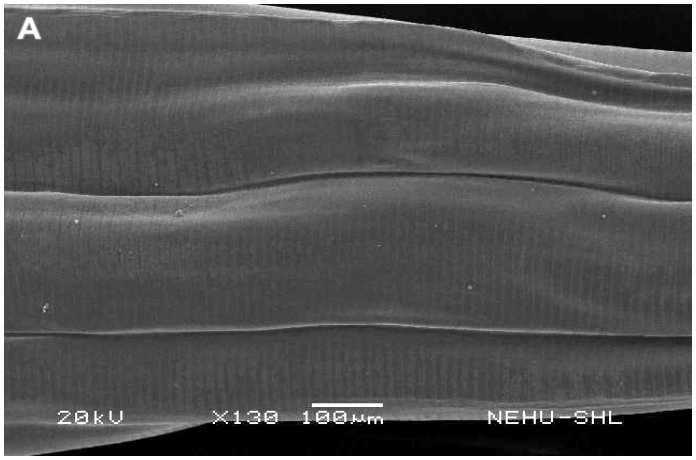

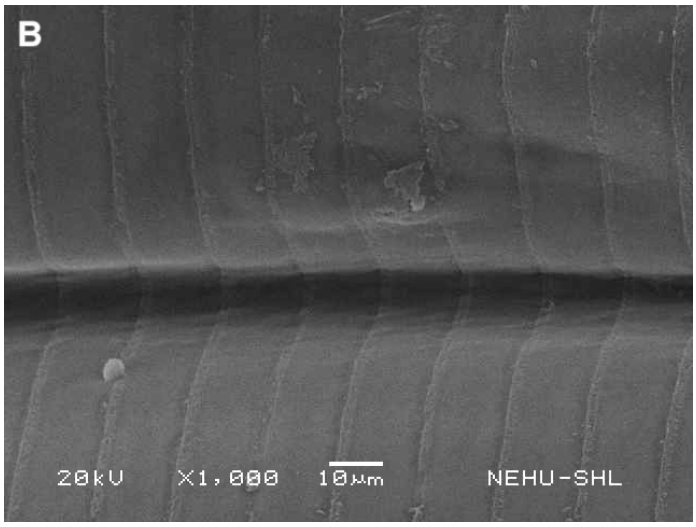

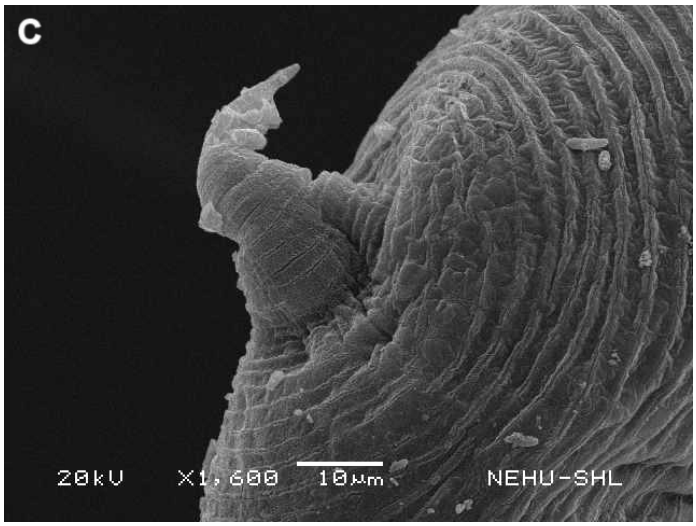

Figure 4: Scanning electron micrograph of *A. galli* treated with 20 mg/mL of *I. khasiana* methanol-hexane extract (IKM-H). (A) Main body showing longitudinal creases due to contractions and fine transverse annulations on the cuticle. (B) Magnification of the cuticle showing patches of scars and erosions. (C) The posterior end indicating continuous contraction and crooked tail end.

Table 5: Compounds identified in *I. khasiana* Methanol-Butanol extract (IKM-B) from GC-MS.

Sl. No.	Retention time (min)	Relative abundance (%)	Compound	Formula	Molecular mass
1	13.94	36.33	Cyclohexan-1,4,5-triol-3-one-1-carboxylic acid.	$C_7H_{10}O_6$	190
2	16.47	34.49	1-Methyl-1-n-octyloxy-1-silacyclobutane.	$C_{12}H_{26}OS$	214
3	17.89	70.74	2,4-Di-tert-butylphenol.	$C_{14}H_{22}O$	206
4	20.18	25.23	Melezitose	$C_{18}H_{32}O_{16}$	504
5	22.49	81.27	7,9-Di-tert-butyl-1-oxaspiro(4,5) deca-6,9-diene-2,8-dione.	$C_{17}H_{24}O_3$	276
6	22.76	64.02	n-Hexadecanoic acid.	$C_{16}H_{32}O_2$	256
7	24.65	11.32	2-Bromotetradecanoic acid.	$C_{14}H_{27}BrO_2$	306
8	26.67	16.50	9-Octadecenoic acid, (2-phenyl-1,3-dioxolan-4-yl) methyl ester.	$C_{28}H_{44}O_4$	444
9	26.91	71.96	Arbutin	$C_{12}H_{16}O_7$	272
10	27.67	37.05	Hexadecanoic acid, 1-(hydroxymethyl)-1,2-ethanediyl ester.	$C_{35}H_{68}O_5$	568
11	29.56	11.81	Androstane-11,17-dione, 3-[(trimethylsilyl)oxy]-, 17-[O-(phenylmethyl)oxime].	$C_{29}H_{43}NO_3Si$	481

Table 6: HPTLC preparation, solvents for mobile phase and reference compounds for different *I. khasiana* extracts.

Sl. No.	Compound	TLC mobile phase	Solvent ratio	Extract in which detected
1	Asiatic acid	Toluene: ethyl acetate: formic acid	5:5:1	-
2	Boswellic acid	Acetic acid: hexane:ethyl acetate: toluene	0.3:1:8:2	-
3	Chebulagic acid	Ethyl acetate: toluene:formic acid: methanol	6:1:1:2	-
4	Chlorogenic acid	Ethyl acetate: dichloromethane: formic acid: acetic acid: water	10:2.5:1:1:1.1	-
5	Ellagic acid	Toluene: ethyl acetate: methanol: formic acid	5:4.5:3:2.5	-
6	Ferulic acid	Toluene: ethyl acetate: formic acid	5:5:0.2	-
7	Gallic acid	Toluene: ethyl acetate: methanol: formic acid	5:4.5:3:2.5	-
8	Quercetin	Toluene: ethyl acetate: formic acid	5:4:0.2	IKM-C
9	β-Sitosterol	Toluene: methanol	16:2	IKM-H

Table 7: HPTLC parameters and validation of standard compounds.

Sl. No.	Parameter	Quercetin	β-sitosterol
1	Linearity (ng/band)	100-500	100-550
2	R_f value	0.48±1	0.43±1
3	Correlation coefficient	0.97	0.99
4	Slope	18.01	3.05
5	Intercept	65.34	209.87
6	Limit of detection (ng/band)	68.01	42.99
7	Limit of quantification (ng/band)	206.07	143.28

Table 8: HPTLC recovery values of bioactive compounds from *I. khasiana* extracts.

Sample	Amount (µL)	Standard compound	Amount (ng/spot)	Expected area	Area obtained	Mean recovery (%)	Relative standard deviation (%)
IKM-C	4	Quercetin	200	11372.13	11230.47	98.75	0.52
	4		300	11721.88	11458.57	97.75	0.46
	4		400	12952.83	12798.83	98.81	0.27
IKM-H	4	β-Sitosterol	200	2867.54	2801.07	97.68	0.31
	4		300	3288.94	3197.32	97.21	0.41
	4		400	3429.34	3388.34	98.80	0.33

Table 9: HPTLC quantification of bioactive compounds in *I. khasiana* extracts.

Sample	R_f value	Mean area (n=1)	Amount (µg)	Regression	Compound
IKM-C	0.48±1	1538.33	0.373	Linear	Quercetin
IKM-H	0.43±1	1558.12	257.04	Linear	β-Sitosterol

Table 10: Anthelmintic susceptibility assay of *I. khasiana* extract against the nematode, *A. galli*.

Media	Dose (mg/mL)	Normalised survival value (h)	*t* value	*t* critical value
Negative control	0	100.00±2.56	-	-
Albendazole	20	001.89±0.52*	182.8	2.37
IKM-H	20	031.73±1.21*	097.8	2.23

As characterised in IKM-C, quercetin is a flavonoid that has been attested as the pharmacological principle of several plants and is known to have broad-spectrum antibacterial, anticancer, antiparasitic, antiviral, cardiovascular protective, hypoglycemic, hypotensive, neuro-protective and anti-immunosuppressive activities.[38,39] Its effectiveness against different Gram-positive and Gram-negative bacteria, pathogenic fungi and viruses has been well documented.[40] It is best understood as a powerful anti-inflammatory molecule. Its anticancer property is reflected by the ability to inhibit mitosis, promote apoptosis, inhibit angiogenesis, suppress metastasis and influence autophagy. It can interfere with signalling molecules such as NRFB, MAPK, AMPK, TGF-β1 and α-SMA, cytokines like cyclooxygenases and lipoxygenases, as well as interleukins like IL-1β, IL-6, TNF-α and NF-κB to induce anti-inflammation at various molecular levels that are linked to cancer development.[41,42]

β-Sitosterol is one of the best understood phytosterols for its chemistry and varied biological activities. It has been profusely recorded to have analgesic, anti-diabetic, anticancer, anti-inflammatory, antimicrobial, antioxidant, hepatoprotective, hypolipidemic, neuro-protective and wound healing effects.[43,44] It is most studied as a promising medication in several cancers including those of breast, colon, leukemia, lung, ovarian, prostate and stomach.[45] Its anticancer activity has been elucidated in different cell lines, showing the ability to interfere with multiple cell signalling pathways involving apoptosis, angiogenesis cell cycle, DNA repair and metastasis.[46,47] It inhibits LEF-1-mediated Wnt/β-catenin pathway, the key molecular pathway in colon cancer development,[48] Vascular Endothelial Growth Factor Receptor 2 (VEGFR2), cell proliferation and inflammatory reactions,[49] while increasing oxidative stress and calcium influx at the endoplasmic reticulum-mitochondria interface.[50] It blocks cell cycle by inhibiting the kinase activity of Cyclin-Dependent Kinase (CDK) to disrupt the cyclin-CDK complexes for further cell proliferation.[47] It also prevents caspase-3 and caspase-9 activation, annexin-V/PI complex, poly (ADP-ribose) polymerase activation, accumulation of matrix metalloproteinases, Bcl-2-Bax interaction and down regulates Trx/Trx1 reductase, while activating P53 to induce cell deaths.[51]

Electron microscopy is the most reliable and precise technique for delineating anthelmintic effects as it reveals the structural alterations on the helminths as drug molecules primarily act on the body surface and the underlying tissues.[24] Each anthelmintic can be identified from the characteristic and signature effects they exert on different body parts of helminths producing distinctive patterns of tissue damages.[25,52] IKM-H was chosen for the anthelmintic assay as it was found to contain the most common and diverse compounds among all the extracts prepared and no less due to its content of 2,6-di-tert-butylphenol and β-sitosterol, which are known to have antiparasitic activity.[53,54] The fine structural changes on the nematode after treatment with IKM-H resulted in unique features, suggesting that the bioactive component(s) may have distinct mode of action. It would be a pertinent endeavour to investigate further for the specific

compounds as the bioactive principle of *I. khasiana*, or whether novel compounds are in obscurity that are yet to be identified as the actual pharmacological molecules. Above all, the study may be perceived as an espousal for conservation of this delicate medicinal plant to comprehensively investigate its true potential health benefits.

CONCLUSION

Chemical profiling of *I. khasiana* leaves using GC-MS revealed the presence of fatty acids, sterols, flavonoids and phenols. 7,9-Di-tert-butyl-1-oxaspiro[4,5]deca-6,9-diene-2,8-dione was the most abundant compound, followed by 6-hydroxy-4,4,7a-trimethyl-5,6,7,7a-tetrahydrobenzofuran-2(4H)-one, 2,4-di-tert-butylphenol and hexadecanoic acid. HPTLC fingerprinting showed the presence of quercetin and β-sitosterol in the chloroform and methanol-hexane extracts respectively. The chemicals identified are all established bioactive compounds against a variety of disease conditions and thereby giving credence to the comprehensive applications of *I. khasiana* in a wide range of ailments in traditional medicines. The plant extract was demonstrated to have anthelmintic efficacy against a nematode parasite. Scanning electron microscopy validated the intricate anthelmintic effects. The findings support the need to conserve this critically endangered plant for further understanding of the underpinning biological modes of action and the exact molecules responsible for the acclaimed medicinal uses.

ACKNOWLEDGEMENT

The study was supported by the DBT-BUILDER (BT/INF/22/SP41398/2021) scheme of the Department of Biotechnology, Government of India.

CONFLICT OF INTEREST

The authors declare that there is no conflict of interest.

ABBREVIATIONS

AMU: Atomic mass unit; **GC-MS:** Gas chromatography-mass spectrometry; **HPTLC:** High-performance thin-layer chromatography; **IKP:** *Ilex khasiana* petroleum ether extract; **IKC:** *Ilex khasiana* chloroform extract; **IKM-H:** *Ilex khasiana* methanol-hexane extract; **IKM-C:** *Ilex khasiana* methanol-chloroform extract; **IKM-B:** *Ilex khasiana* methanol-butanol extract; **LOD:** Limit of detection; **LOQ:** Limit of quantification; **TLC:** Thin-layer chromatography.

DATA AVAILABILITY

Additional data used to support the findings of this study are included in the supplementary file.

SUMMARY

Five different extracts of *Ilex khasiana*, namely Petroleum ether extract (IKP), Chloroform extract (IKC), Methanol-Hexane extract (IKM-H), Methanol-Chloroform extract (IKM-C) and Methanol-Butanol extract (IKM-B) were prepared from the leaves by Soxhlet extraction. Chemical analysis using gas chromatography-mass spectrometry showed the presence of important bioactive compounds including fatty acids, sterols, flavonoids and phenols. Quercetin and β-sitosterol were quantified using HPTLC. Quercetin was estimated at 372.98 ng in IKM-C and β-sitosterol at 257.04 ng in IKM-H. The plant extract exhibits anthelmintic activity against an intestinal nematode. Characteristic anthelmintic damages were revealed by scanning electron microscopy.

REFERENCES

1. Mir AH, Upadhaya K, Roy DK, Deori C, Singh B. A comprehensive checklist of endemic flora of Meghalaya, India. J Threat Taxa. 2019;11(12):14527-61. doi: 10.11609/jott.4605.11.12.14527-14561.
2. Purkayastha CS. Four new species from Assam. Indian For. 1938;64(5):277-8.
3. Lalnunfela C, Lalremsanga HT, Lalhriatpuii TC, Lalnunzira D, Lalchhandama K. Unveiling the unexplored and critically endangered *Ilex khasiana* for its antioxidant properties. J Nat Remedies. 2019:214-20. doi: 10.18311/jnr/2019/23671.
4. Adhikari D, Barik SK, Upadhaya K. Habitat distribution modelling for reintroduction of *Ilex khasiana* Purk., a critically endangered tree species of northeastern India. Ecol Eng. 2012;40:37-43. doi: 10.1016/j.ecoleng.2011.12.004.
5. Krishna U, Kanta BS, Dibyendu A, Ratul B, John LN. Regeneration ecology and population status of a critically endangered and endemic tree species (*Ilex khasiana* Purk.) in north-eastern India. J Forest Res. 2009;20:223-8. doi: 10.1093/aobpla/plr012.
6. Lalnunfela C, Lalthanpuii PB, Lalhriatpuii TC, Lalchhandama K. An endangered medicinal plant, *Ilex khasiana* exhibits potent antiparasitic activity against intestinal tapeworm. Pharmacogn J. 2020;12(4):725-30. doi: 10.5530/pj.2020.12.105.
7. Lalnunfela C, Lalremsanga HT, Lalchhandama K, Lalthanpuii PB, Lalmuanthanga C, Lalhriatpuii TC. *In vivo* evaluation of *Ilex khasiana* for its analgesic and anti-inflammatory activity on Swiss albino mice model. Indian J Sci Technol. 2023;16:39-47. doi: 10.17485/IJST/v16sp1.msc6.
8. Noureddine T, El Husseini Z, Nehme A, Massih RA. Antibacterial activity of *Ilex paraguariensis* (Yerba Mate) against Gram-positive and Gram-negative bacteria. J Infect Dev Countr. 2018;12(09):712-9. doi: 10.3855/jidc.10380.
9. Yao X, Zhang F, Corlett RT. Utilization of the hollies (*Ilex* L. spp.): A review. Forests. 2022;13(1):94. doi: 10.3390/f13010094.
10. Gawron-Gzella A, Chanaj-Kaczmarek J, Cielecka-Piontek J. Yerba mate-a long but current history. Nutrients. 2021;13(11):3706. doi: 10.3390/nu13113706.
11. Bastos DH, Saldanha LA, Catharino RR, Sawaya AC, Cunha IB, Carvalho PO, Eberlin MN. Phenolic antioxidants identified by ESI-MS from yerba mate (*Ilex paraguariensis*) and green tea (*Camelia sinensis*) extracts. Molecules. 2007;12(3):423-32. doi: 10.3390/12030423.
12. Alam M, Ahmed S, Elasbali AM, Adnan M, Alam S, Hassan MI, Pasupuleti VR. Therapeutic implications of caffeic acid in cancer and neurological diseases. Front Oncol. 2022;12:860508. doi: 10.3389/fonc.2022.860508.
13. Amigo-Benavent M, Wang S, Mateos R, Sarriá B, Bravo L. Antiproliferative and cytotoxic effects of green coffee and yerba mate extracts, their main hydroxycinnamic acids, methylxanthine and metabolites in different human cell lines. Food Chem Toxicol. 2017;106:125-38. doi: 10.1016/j.fct.2017.05.019.
14. de Mejía EG, Song YS, Heck CI, Ramírez-Mares M. Yerba mate tea (*Ilex paraguariensis*): Phenolics, antioxidant capacity and *in vitro* inhibition of colon cancer cell proliferation. J Funct Foods. 2010;2(1):23-34. doi: 10.1016/j.jff.2009.12.003.
15. Li L, Xu LJ, Ma GZ, Dong YM, Peng Y, Xiao PG. The large-leaved Kudingcha (*Ilex latifolia* Thunb and *Ilex kudingcha* CJ Tseng): a traditional Chinese tea with plentiful secondary metabolites and potential biological activities. J Nat Med. 2013;67:425-37. doi: 10.1007/s11418-013-0758-z.
16. Hao D, Gu X, Xiao P, Liang Z, Xu L, Peng Y. Research progress in the phytochemistry and biology of *Ilex* pharmaceutical resources. Acta Pharm Sin B. 2013;3(1):8-19. doi: 10.1016/j.apsb.2012.12.008.
17. Jiang S, Cui H, Wu P, Liu Z, Zhao Z. Botany, traditional uses, phytochemistry, pharmacology and toxicology of *Ilex pubescens* Hook et Arn. J Ethnopharmacol. 2019;245:112147. doi: 10.1016/j.jep.2019.112147.

18. Liao L, Zhou X, Liu YL, Xu QM, Li XR, Yang SL. Four new triterpenoidal saponins from *Ilex cornuta* and their cytotoxic activities. Phytochem Lett. 2013;6(3):429-34. doi: 10.1016/j.phytol.2013.05.013.
19. Si-Xiang ZH, Zhi-Rong YA, Jun LI, Peng-Fei TU. Flavonoids from the leaves of *Ilex cornuta*. Chin J Nat Med. 2012;10(2):84-7. doi: 10.3724/SP.J.1009.2012.00084.
20. Zuo WJ, Mei WL, Zeng YB, Wang H, Dai HF. Research advances on the chemical constituents and pharmacological activities of *Ilex cornuta* Lindl. et Paxt. Med Plant. 2011;2:69-71.
21. Cheng G, Zhang JH, Yuan H, Zheng B, Yan D. Research progress of chemical constituents and pharmacological effects of common medicinal plants of *Ilex*. Chin Agric Sci Bull, 2024;40(8):30-37. doi: 10.11924/j.issn.1000-6850.casb2023-031
22. Tyihák E, Mincsovics E, Kalász H. New planar liquid chromatographic technique: over pressured thin-layer chromatography. J Chromatogr A. 1979;174(1):75-81. doi: 10.1016/S0021-9673(00)87038-7.
23. Renger B. Contemporary thin-layer chromatography in pharmaceutical quality control. J AOAC Int. 1998;81(2):333-40. doi: 10.1093/jaoac/81.2.333.
24. Lalchhandama K. *In vitro* effects of albendazole on *Raillietina echinobothrida*, the cestode of chicken, *Gallus domesticus*. J Young Pharm. 2010;2(4):374-8. doi: 10.4103/0975-1483.71630.
25. Lalthanpuii PB, Lalchhandama K. Scanning electron microscopic study of the anthelmintic effects of some anthelmintic drugs on poultry nematode, *Ascaridia galli*. Adv Anim Vet Sci. 2020;8(8):788-93. doi: 10.17582/journal.aavs/2020/8.8.788.793.
26. Kumar S, Arif M, Jawaid T, Al-Khamees OA, Anjum A, Shafi S, *et al.* Antiplatelet and thrombolytic activity of phenolic-insistent fractions from the new-fangled stem of *Ficus benghalensis* with concurrent GC-MS analysis. Intell Pharm. 2023;1(4):224-31. doi: 10.1016/j.ipha.2023.07.005.
27. Lakshmegowda SB, Rajesh SK, Kandikattu HK, Nallamuthu I, Khanum F. *In vitro* and *in vivo* studies on hexane fraction of *Nitzschia palea*, a freshwater diatom for oxidative damage protective and anti-inflammatory response. Rev Bras Farmacogn. 2020;30:189-201. doi: 10.1007/s43450-020-00008-6.
28. Tavanappanavar AN, Mulla SI, Seth CS, Bagewadi ZK, Rahamathulla M, Ahmed MM, *et al.* Phytochemical analysis, GC-MS profile and determination of antibacterial, antifungal, anti-inflammatory, antioxidant activities of peel and seeds extracts (chloroform and ethyl acetate) of *Tamarindus indica* L. Saudi J Biol Sci. 2024;31(1):103878. doi: 10.1016/j.sjbs.2023.103878
29. Taher MA, Laboni AA, Shompa SA, Rahman MM, Hasan MM, Hasnat H, *et al.* Bioactive compounds extracted from leaves of *G. cyanocarpa* using various solvents in chromatographic separation showed anti-cancer and anti-microbial potentiality in *in silico* approach. Chin J Anal Chem. 2023;51(12):100336. doi: 10.1016/j.cjac.2023.100336.
30. Jayawardena TU, Kim HS, Sanjeewa KA, Han EJ, Jee Y, Ahn G, *et al.* Loliolide, isolated from *Sargassum horneri*; abate LPS-induced inflammation via TLR mediated NF-κB, MAPK pathways in macrophages. Algal Res. 2021;56:102297. doi: 10.1016/j.algal.2021.102297.
31. Tatipamula VB, Ketha A, Nallapaty S, Kottana H, Koneru ST. Moss *Octoblepharum albidum* Hedw.: Isolation, characterization, *in vitro* and *in vivo* antidiabetic activities. Adv Trad Med. 2021;21:351-60. doi: 10.1007/s13596-021-00556-9.
32. Zhao F, Wang P, Lucardi RD, Su Z, Li S. Natural sources and bioactivities of 2, 4-di-tert-butylphenol and its analogs. Toxins. 2020;12(1):35. doi: 10.3390/toxins12010035.
33. Kar K, Ghosh D, Kabi B, Chandra A. A concise review on cobalt Schiff base complexes as anticancer agents. Polyhedron. 2022;222:115890. doi: 10.1016/j.poly.2022.115890.
34. Antonenko TA, Shpakovsky DB, Vorobyov MA, Gracheva YA, Kharitonashvili EV, Dubova LG, *et al.* Antioxidative vs cytotoxic activities of organotin complexes bearing 2, 6-di-tert-butylphenol moieties. Appl Organomet Chem. 2018;32(7):e4381. doi: 10.1002/aoc.4381.
35. Aparna V, Dileep KV, Mandal PK, Karthe P, Sadasivan C, Haridas M. Anti-inflammatory property of n-hexadecanoic acid: structural evidence and kinetic assessment. Chem Biol Drug Des. 2012;80(3):434-9. doi: 10.1111/j.1747-0285.2012.01418.x.
36. Bharath B, Perinbam K, Devanesan S, AlSalhi MS, Saravanan M. Evaluation of the anticancer potential of hexadecanoic acid from brown algae *Turbinaria ornata* on HT–29 colon cancer cells. J Mol Struct. 2021; 1235:130229. doi: 10.1016/j.molstruc.2021.130229.
37. Ganesan T, Subban M, Christopher Leslee DB, Kuppannan SB, Seedevi P. Structural characterization of n-hexadecanoic acid from the leaves of *Ipomoea eriocarpa* and its antioxidant and antibacterial activities. Biomass Convers Bioref. 2022;30:1-2. doi: 10.1007/s13399-022-03576-w.
38. Azeem M, Hanif M, Mahmood K, Ameer N, Chughtai FR, Abid U. An insight into anticancer, antioxidant, antimicrobial, antidiabetic and anti-inflammatory effects of quercetin: A review. Polym Bull. 2023;80(1):241-62. doi: 10.1007/s00289-022-04091-8.
39. Hosseini A, Razavi BM, Banach M, Hosseinzadeh H. Quercetin and metabolic syndrome: A review. Phytother Res. 2021;35(10):5352-64. doi: 10.1002/ptr.7144.
40. Nguyen TL, Bhattacharya D. Antimicrobial activity of quercetin: an approach to its mechanistic principle. Molecules. 2022;27(8):2494. doi: 10.3390/molecules27082494.
41. Tang SM, Deng XT, Zhou J, Li QP, Ge XX, Miao L. Pharmacological basis and new insights of quercetin action in respect to its anti-cancer effects. Biomed Pharmacother. 2020;121:109604. doi: 10.1016/j.biopha.2019.109604.
42. Zhou Y, Qian C, Tang Y, Song M, Zhang T, Dong G, *et al.* Advance in the pharmacological effects of quercetin in modulating oxidative stress and inflammation related disorders. Phytother Res. 2023;37(11):4999-5016. doi: 10.1002/ptr.7966.
43. Babu S, Jayaraman S. An update on β-sitosterol: A potential herbal nutraceutical for diabetic management. Biomed Pharmacother. 2020;131:110702. doi: 10.1016/j.biopha.2020.110702.
44. Yadav P, Chauhan C, Singh S, Banerjee S, Murti K. β-Sitosterol in various pathological conditions: An update. Curr Bioact Comp. 2022;18(6):19-27. doi: 10.2174/1573407218666211230144036.
45. Nandi S, Nag A, Khatua S, Sen S, Chakraborty N, Naskar A, Acharya K, Calina D, Sharifi-Rad J. Anticancer activity and other biomedical properties of β-sitosterol: Bridging phytochemistry and current pharmacological evidence for future translational approaches. Phytother Res. 2024;38(2):592-619. doi: 10.1002/ptr.8061.
46. Khan Z, Nath N, Rauf A, Emran TB, Mitra S, Islam F, *et al.* Multifunctional roles and pharmacological potential of β-sitosterol: Emerging evidence toward clinical applications. Chem Biol Interact. 2022;365:110117. doi: 10.1016/j.cbi.2022.110117.
47. Bao X, Zhang Y, Zhang H, Xia L. Molecular mechanism of β-sitosterol and its derivatives in tumor progression. Front Oncol. 2022;12:926975. doi: 10.3389/fonc.2022.926975.
48. Gu S, Liu F, Xie X, Ding M, Wang Z, Xing X, *et al.* β-Sitosterol blocks the LEF-1-mediated Wnt/β-catenin pathway to inhibit proliferation of human colon cancer cells. Cell Signal. 2023;104:110585. doi: 10.1016/j.cellsig.2022.110585.
49. Qian K, Zheng XX, Xu SD. β-Sitosterol inhibits rheumatoid synovial angiogenesis through suppressing VEGF signaling pathway. Front Pharmacol. 2022;12:816477. doi: 10.3389/fphar.2021.816477.
50. Bae H, Park S, Ham J, Song J, Hong T, Choi JH, *et al.* ER-mitochondria calcium flux by β-sitosterol promotes cell death in ovarian cancer. Antioxidants. 2021;10(10):1583. doi: 10.3390/antiox10101583.
51. Rajavel T, Packiyaraj P, Suryanarayanan V, Singh SK, Ruckmani K, Pandima Devi K. β-Sitosterol targets Trx/Trx1 reductase to induce apoptosis in A549 cells via ROS mediated mitochondrial dysregulation and p53 activation. Sci Rep. 2018;8(1):2071. doi: 10.1038/s41598-018-20311-6.
52. Lalthanpuii PB, Zokimi Z, Lalchhandama K. Anthelmintic activity of praziquantel and *Spilanthes acmella* extract on an intestinal cestode parasite. Acta Pharm. 2020;70(4):551-60. doi: 10.2478/acph-2020-0039
53. Roy D, Anas M, Manhas A, Saha S, Kumar N, Panda G. Synthesis, biological evaluation, structure-activity relationship studies of quinoline-imidazole derivatives as potent antimalarial agents. Bioorg Chem. 2022;121:105671. doi: 10.1016/j.bioorg.2022.105671.
54. Pineda-Alegría JA, Sánchez JE, González-Cortazar M, Von Son-De Fernex E, González-Garduño R, Mendoza-de Gives P, et al. *In vitro* nematocidal activity of commercial fatty acids and β-sitosterol against *Haemonchus contortus*. J Helminthol. 2020;94:e135. doi: 10.1017/S0022149X20000152.

Cite this article: Lalnunfela C, Lalthanpuii PB, Lalremsanga HT, Lalhriatpuii TC, Lalchhandama K. Chemical Profiling, Chromatographic Fingerprinting and Anthelmintic Screening of a Rare Species of Holly, *Ilex khasiana* Purkay. from Mizoram, Northeast India. Pharmacog Res. 2024;16(4):757-68.

SUPPLEMENTARY FILE

Chemical profiling, chromatographic fingerprinting and anthelmintic screening of a rare species of holly, *Ilex khasiana* Purkay., from Mizoram, Northeast India

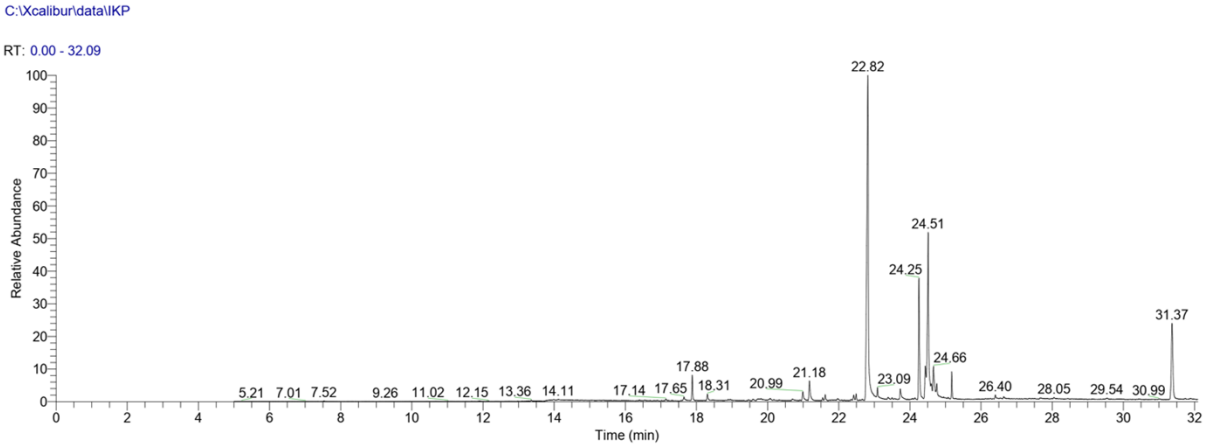

Figure S1: Chromatogram of compounds detected in *I. khasiana* Petroleum ether extract (IKP) from gas chromatography-mass spectrometry. Corresponding compounds are listed in Table 1.

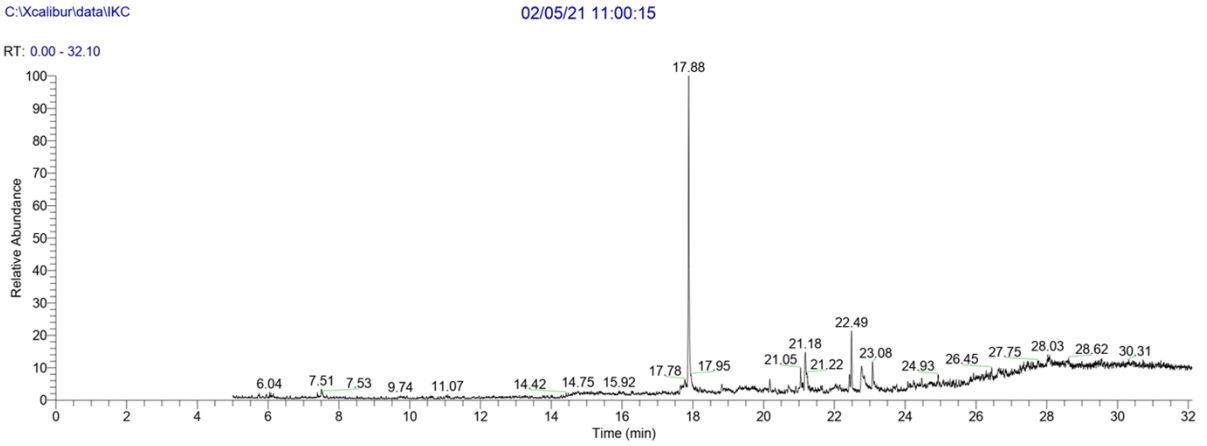

Figure S2: Chromatogram of compounds detected in *I. khasiana* Chloroform Extract (IKC) from gas chromatography-mass spectrometry. Corresponding compounds are listed in Table 2.

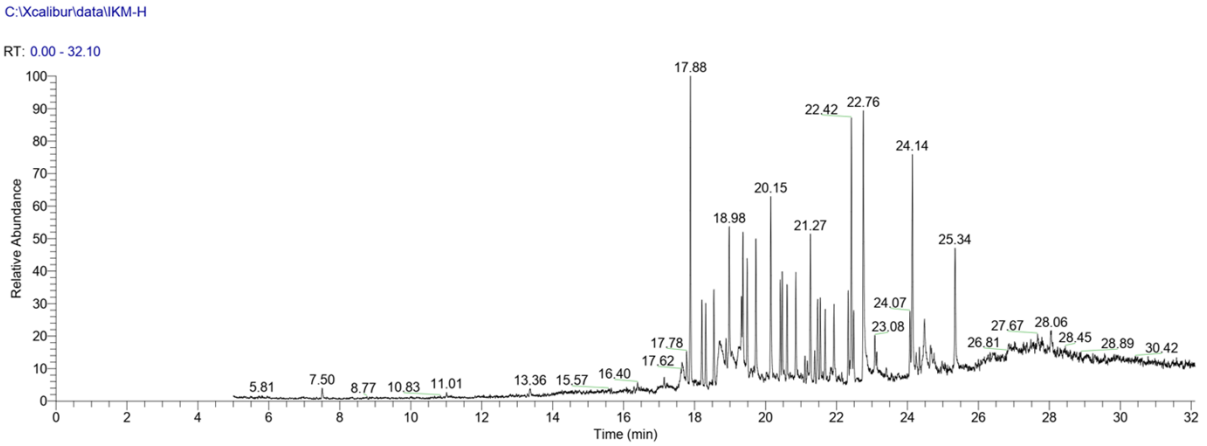

Figure S3: Chromatogram of compounds detected in *I. khasiana* Methanol-Hexane extract (IKM-H) from gas chromatography-mass spectrometry. Corresponding compounds are listed in Table 3.

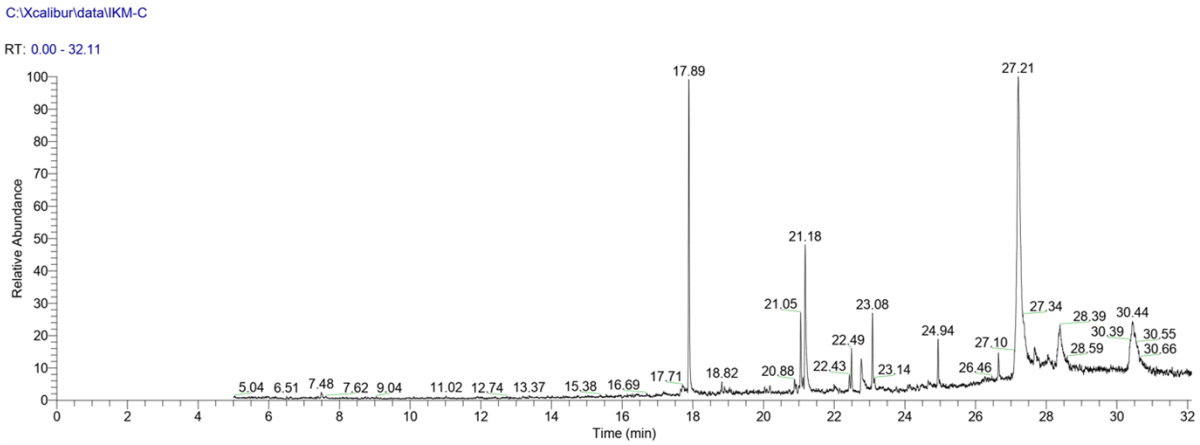

Figure S4: Chromatogram of compounds detected in *I. khasiana* Methanol-Chloroform extract (IKM-C) from gas chromatography-mass spectrometry. Corresponding compounds are listed in Table 4.

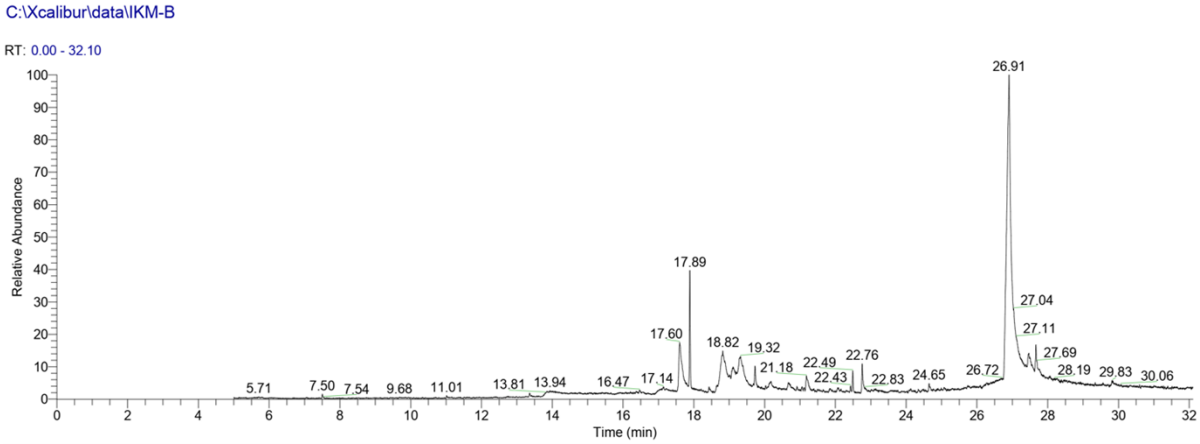

Figure S5: Chromatogram of compounds detected in *I. khasiana* Methanol-Butane extract (IKM-B) from gas chromatography-mass spectrometry. Corresponding compounds are listed in Table 5.

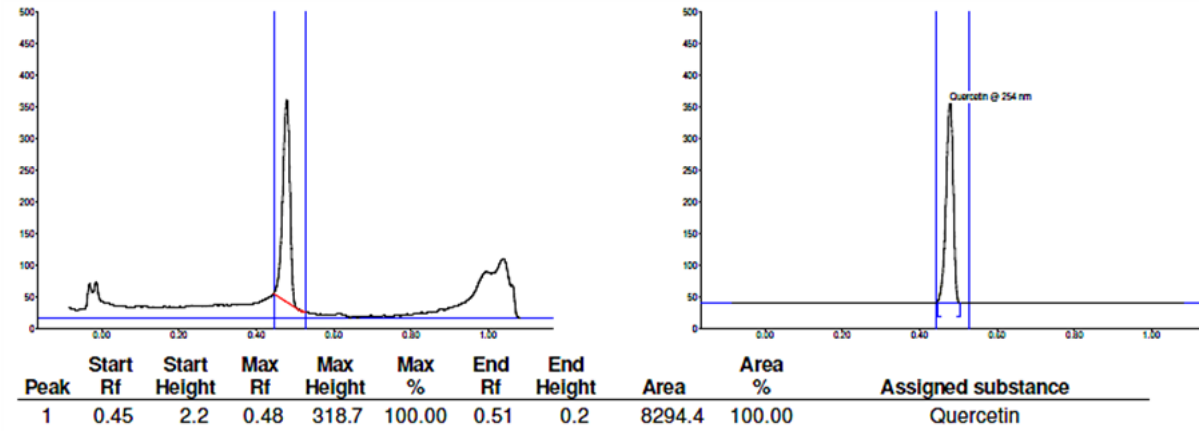

Peak	Start Rf	Start Height	Max Rf	Max Height	Max %	End Rf	End Height	Area	Area %	Assigned substance
1	0.45	2.2	0.48	318.7	100.00	0.51	0.2	8294.4	100.00	Quercetin

Figure S6: HPTLC chromatogram profile of standard quercetin detected at 254 nm and its respective R_f value.

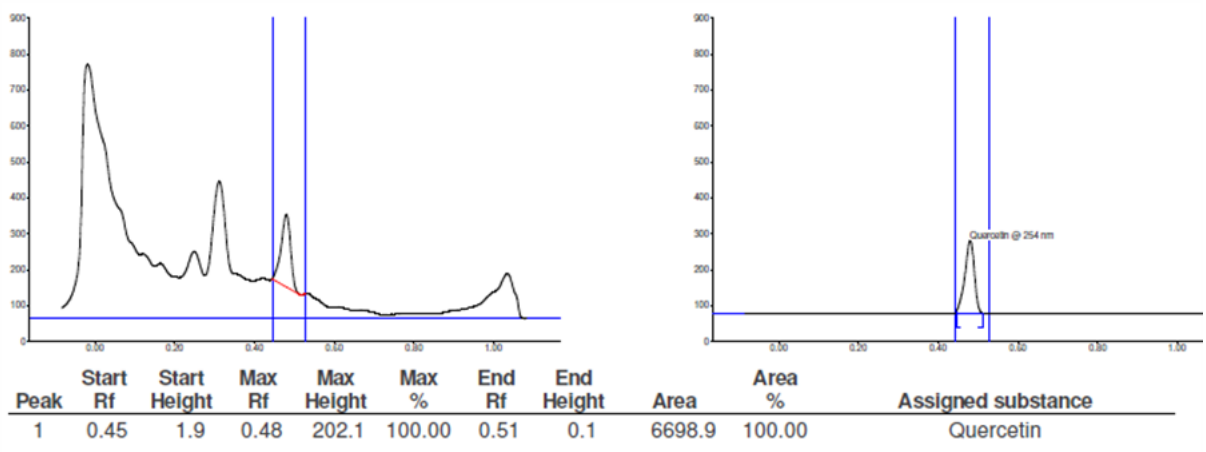

Peak	Start Rf	Start Height	Max Rf	Max Height	Max %	End Rf	End Height	Area	Area %	Assigned substance
1	0.45	1.9	0.48	202.1	100.00	0.51	0.1	6698.9	100.00	Quercetin

Figure S7: HPTLC chromatogram profile of quercetin in *I. khasiana* Methanol-Chloroform extract (IKM-C) detected at 254 nm and an Rf value of 0.49.

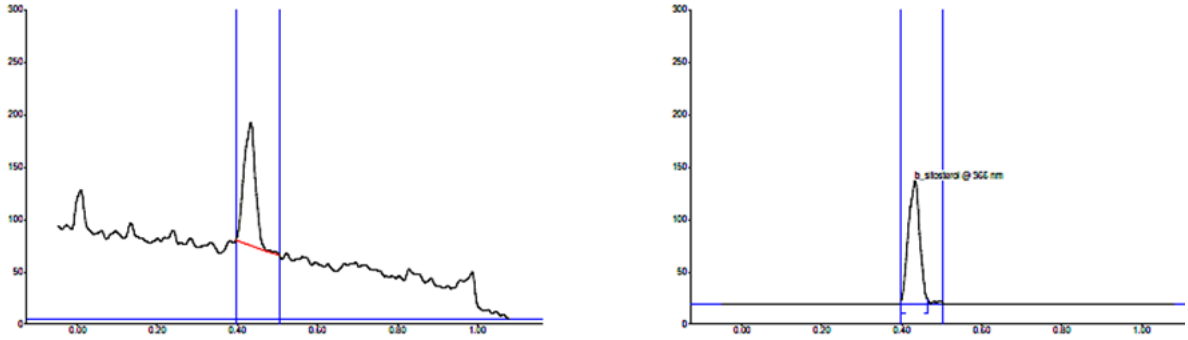

Peak	Start Rf	Start Height	Max Rf	Max Height	Max %	End Rf	End Height	Area	Area %	Assigned substance
1	0.40	1.9	0.43	117.3	100.00	0.47	3.7	2386.2	100.00	b_sitosterol

Figure S8: HPTLC chromatogram profile of standard β-sitosterol detected at 366 nm and its respective R_f value.

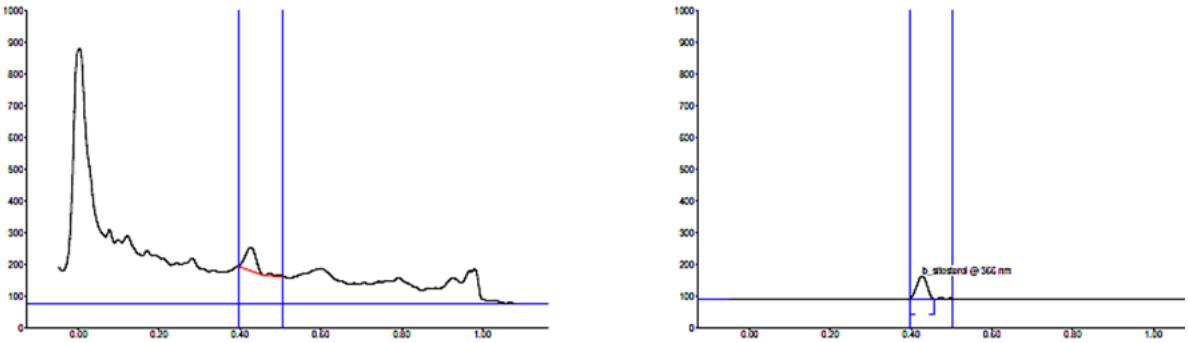

Peak	Start Rf	Start Height	Max Rf	Max Height	Max %	End Rf	End Height	Area	Area %	Assigned substance
1	0.40	1.7	0.43	74.8	100.00	0.46	0.0	1378.6	100.00	b_sitosterol

Figure S9: HPTLC chromatogram profile of β-sitosterol in *I. khasiana* Methanol-Hexane extract (IKM-H) detected at 254 nm and at an R_f value of 0.43.